

# Exploring Self-Supervised Skeleton-Based Human Action Recognition under Occlusions

Yifei Chen  
KIT, Germany  
cyf236510120@gmail.com

Kunyu Peng\*  
KIT, Germany  
kunyu.peng@kit.edu

Alina Roitberg  
Stuttgart University, Germany  
alina.roitberg@ki.uni-stuttgart.de

David Schneider  
KIT, Germany  
david.schneider@kit.edu

Jiaming Zhang  
KIT, Germany  
jiaming.zhang@kit.edu

Junwei Zheng  
KIT, Germany  
junwei.zheng@kit.edu

Yufan Chen  
KIT, Germany  
yufan.chen@kit.edu

Ruiping Liu  
KIT, Germany  
ruiping.liu@kit.edu

Kailun Yang  
Hunan University, China  
kailun.yang@hnu.edu.cn

Rainer Stiefelhagen  
KIT, Germany  
rainer.stiefelhagen@kit.edu

**Abstract**—To integrate self-supervised skeleton-based action recognition methods into autonomous robotic systems, it is crucial to consider adverse situations involving target *occlusions*. Such a scenario, despite its practical relevance, is rarely addressed in existing self-supervised skeleton-based action recognition methods. To empower models with the capacity to address occlusion, we propose a simple and effective method. We first pre-train using occluded skeleton sequences, then use k-means clustering (KMeans) on sequence embeddings to group semantically similar samples. Next, we propose KNN-Imputation to fill in missing skeleton data based on the closest sample neighbors. Imputing incomplete skeleton sequences to create relatively complete sequences as input provides significant benefits to existing skeleton-based self-supervised methods. Meanwhile, building on the state-of-the-art Partial Spatio-Temporal Learning (PSTL), we introduce an Occluded Partial Spatio-Temporal Learning (OPSTL) framework. This enhancement utilizes Adaptive Spatial Masking (ASM) for better use of high-quality, intact skeletons. The new proposed method is verified on the challenging occluded versions of the NTURGB+D 60 and NTURGB+D 120. The source code is publicly available at <https://github.com/cyfml/OPSTL>.

**Index Terms**—Self-supervised skeleton-based human action recognition, human action recognition under occlusions.

## I. INTRODUCTION

Human action recognition has extensive applications in the field of robotics, such as human-robot interaction, healthcare, industrial automation, security, and surveillance [1]–[17].

In particular, robots can collaborate with humans as partners, assist them in various tasks by identifying human actions and needs, and take care of patients. The capability to understand human intentions and goals allows a robot to discern when its assistance is most needed, thereby minimizing disruptions to human activities. A robot equipped with a human action recognition system can also be used to monitor the condition of patients to provide better daily-life assistance for their recovery [18], [19], assess the safety of its surroundings, issue warnings, and detect gestures for help in rescue missions to provide assistance. Challenges of

image- or video-based action recognition [20] stem from multiple factors: complex backgrounds, variations in human body shapes, changing viewpoints, or motion speed alterations. In contrast to video-based action recognition [21]–[23], skeleton-based action recognition is less sensitive to appearance factors and has the advantage of superior efficiency by using sparse 3D skeleton data as input, which ensures fast inference speed and small memory usage. Thanks to the advancement of depth sensors [24] and lightweight and robust pose estimation algorithms [25], [26], obtaining high-quality skeleton data is becoming easier. Skeleton-based action recognition has rapidly progressed in recent years. Its efficiency designates it for mobile robots with computational constraints, at the same time self-supervised solutions [27], [28] have gradually grasped the attention of the robot research community since this technique allows for training such methods with little annotation effort.

The majority of existing work on self-supervised skeleton-based action recognition [29]–[33] is conducted on occlusion-free data collected in well-constrained environments. In practice, robots often encounter occluded environments in the real world, even high-quality pose detectors can not provide reliable full-body poses in such situations. For this reason, we argue that occlusion-aware training and evaluation is an overlooked but crucial task in this field. The occlusion problem in self-supervised skeleton-based action recognition can be considered from two points of view. On one hand, it can be addressed by improving the robustness of the model to occlusion by manipulating the model architecture, and on the other hand, it can be handled through the data itself and completing the missing skeleton coordinates as much as possible.

In this work, we for the first time tackle the self-supervised skeleton-based action recognition task under occlusions. A benchmark is firstly built by introducing the occlusion derived from Peng *et al.* [34]. On this benchmark, obvious performance decays are observed when using occluded skeleton data on all existing methods. We thereby contribute a new method

\* corresponding author

by considering both model- and data perspectives, and then evaluate the proposed solution on this benchmark.

From the model perspective, we introduce a novel dataset-driven *Adaptive Spatial Masking (ASM)* data augmentation based on the current state-of-the-art approach, *i.e.*, PSTL [32] and name the new self-supervised skeleton-based human action recognition framework as OPSTL. ASM masks joints based on the distribution of missing joints within the dataset to effectively leverage intact data to learn feature representation. For the data-driven approach, we propose a simple but effective method that enhances the performance of existing popular self-supervised action recognition methods for downstream tasks by completing missing data. Intuitively, one might search for similar dataset samples to fill in missing data. However, due to the vast amount of data and the density of the original skeleton data, directly applying KNN [35] to search for neighboring samples is highly impractical and unacceptable in terms of both time and space considerations.

To improve computational efficiency, we propose a two-stage approach. In the first stage, samples are grouped into distinct categories through KMeans [36] clustering on features learned through self-supervised learning methods. In the second stage, missing values are imputed by leveraging close neighbors within the same cluster. The proposed approach eliminates the need for a KNN search on the entire dataset during the imputation process. Instead, KNN imputation is applied within each smaller cluster, leading to a considerable reduction in computational overhead. We summarize our contributions as follows:

- To investigate robotic action recognition performance in difficult environments, a large-scale occlusion-based benchmark is constructed for self-supervised skeleton-based action recognition, including both NTU-60 and NTU-120 datasets.
- Our work contains two technical contributions to alleviate the perturbation from occlusion, where a two-stage imputation method using KMeans and KNN to reduce computation overhead for the occluded skeleton completion (KNN-Imputation) and a novel dataset-driven *Adaptive Spatial Masking (ASM)* data augmentation to achieve Occluded Partial Spatio-Temporal Learning (OPSTL) are proposed. The proposed techniques show superior performances on the occlusion challenge for skeleton-based human action recognition.

## II. METHODOLOGY

### A. Pre-processing

A pre-processed skeleton sequence can be represented as  $s \in \mathbb{R}^{C \times T \times V}$  from the original input  $I \in \mathbb{R}^{C \times T \times V \times M}$ .  $T$  is the frame number and  $V$  is the joint number.  $C$  denotes the channel number.  $M$  represents the person number. The preprocessing is similar to that of CrosSCLR [30]. Skeleton coordinates are relative coordinates, relative to the center joint of the skeleton. Additionally, we need to compute the missing joint boolean matrix ( $\mathbf{B} \in \mathbb{B}^{N \times V}$ ) of the  $V$  joints for each

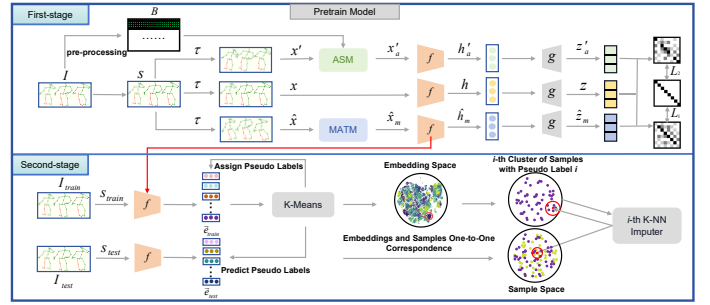


Fig. 1: An overview of the proposed approach.

sample to better mask the joints that are more occluded in the ASM mechanism. The coordinates of all missing joints will be represented as “nan”, which facilitates the subsequent calculation of Euclidean distances with missing values during imputation.

### B. Partial Spatio-Temporal Skeleton Representation Learning

Many existing methods [30], [31] focus on generating various views of skeleton sequences for contrastive learning, but they often overlook the local relationships between different skeleton joints and frames. However, these local relationships are vital for real-world applications because they provide critical context for tasks like action recognition. To bridge this gap, PSTL [32] leverages local relationships by using a unique spatiotemporal masking strategy to create partial skeleton sequences. These sequences are utilized in a triplet stream structure comprising an anchor stream, a spatial masking stream with Central Spatial Masking (CSM), and a temporal masking stream with Motion Attention Temporal Masking (MATM). Therefore, PSTL shows a certain level of effectiveness in handling occlusion. PSTL adopts the framework of Barlow Twins [33], thus avoiding the drawbacks of contrastive learning that require a large number of negative samples, as well as the need for a large batch size and memory bank [30], [31].

### C. Adaptive Spatial Masking

The self-supervised skeleton-based action recognition method, PSTL [32], employs Central Spatial Masking (CSM) to enhance the robustness of the learned representation with respect to joints. However, it does not take into account considering the actual occlusion situation. When only some joints of each sample are occluded, we can choose to mask the joints with higher occlusion frequency in the training set to better utilize high-quality data for learning. On the other hand, when each sample is randomly occluded with a higher occlusion rate, the masking strategy should also shift from a fixed strategy to a random mask, in order to better simulate the distribution of occlusions. Therefore, we propose dataset-driven Adaptive Spatial Masking (ASM), which can adaptively switch between partial occlusion and random occlusion. It is worth noting that we still retain CSM in ASM. When no joints are occluded in this batch, we still use CSM to select joints for masking. We redefine the degree of each joint based on the

missing joint boolean matrix ( $\mathbf{B}$ ) in each batch. The missing frequency of each joint  $v_i$ ,  $i \in (1, 2, \dots, n)$  is calculated within each batch. The Frequency Degree (FD) of joint  $v_i$  can be formulated as:

$$FD_i = \lfloor \frac{F_i - \min(F)}{\max(F) - \min(F) + \epsilon} \times 3 + 1 \rfloor, \quad (1)$$

where  $\epsilon$  is a small value of 0.001. We observed that the majority of joints have a degree of around 2, and the differences in degrees are relatively small. Consequently, the performance difference between random masking and degree-based masking is not significant. Thus, we rescale the frequency of each joint's occlusion to a range similar to the degrees, *i.e.*, [1, 3]. Due to the larger differences in frequency degrees generated by this rescaling compared to the degree of centrality of the human skeleton graph topology, the joint masking tends to favor joints with a higher frequency of occlusion. Here  $F$  is the frequency of missing joints computed on  $\mathbf{B}$  along the batch dimension  $b$ :

$$F_i = \sum_b \mathbf{B}_{b,i}. \quad (2)$$

#### D. KNN Imputation

We aim to find the most similar samples to the ones with missing values for imputation. However, due to the high dimensionality and large amount of sample data, directly searching for neighbors in the sample space is impractical. Therefore, we consider it unnecessary to search the entire sample space. Instead, we divide the samples into clusters with fewer skeleton samples. Through the first stage of pre-training, KMeans can roughly cluster samples with the same action type into a cluster.

Firstly, we need to use the pre-trained model from the first stage to extract features from the samples. The extracted embeddings  $\vec{e}_{train} \in \mathbf{R}^{N \times D}$ , where  $N$  is the number of samples in the training set and  $D$  is the dimension of embeddings, are clustered using KMeans, and pseudo-labels are assigned to each embedding. Since there is a one-to-one correspondence between embeddings and original samples, each sample is also assigned a pseudo-label. For a given cluster of samples with pseudo label  $i$ , we utilize KNN to search for neighboring samples of the sample that need imputation within the same cluster. Because these neighboring samples may also have missing values, the standard Euclidean distance is not applicable. Here, we use a modified Euclidean distance based on missing values [37], [38], which is formulated as:

$$dist(S_{ij}, S_{ik}) = \sqrt{w \times d_{ignore}(S_{ij}, S_{ik})}, \quad (3)$$

where  $w$  is a weight that can be expressed as the ratio of the total number of coordinates to the number of present coordinates, and  $d_{ignore}(S_{ij}, S_{ik})$  is the Euclidean distance between sample  $j$  and sample  $k$  in  $i$ -th cluster that ignores missing values in  $S_{ij}$  and  $S_{ik}$ .

Based on this distance metric, it is straightforward to compute distances between each pair of samples. The nearest  $k$  samples  $S_{ij}^{near}$ ,  $j \in (1, 2, \dots, k)$  are selected based on distance and missing position from the current cluster  $i$  for one of the

samples with missing data  $S_i^{miss}$ , and each sample  $S_{ij}^{near}$  should have intact coordinate  $C_j$  at the position  $p \in \mathbb{Z}^{T \times V \times M}$  where missing coordinates  $C_i^{miss} = \{c \mid c \in S_i^{miss}\}$  occur. The imputation formula for a missing skeleton coordinate of a missing sample is given as:

$$C_m^{miss} = \frac{\sum_{j=1}^k r_j \times C_j}{\sum_{j=1}^k r_j}, m \in (1, 2, \dots, n), \quad (4)$$

where  $r_j$  is the reciprocal of the modified Euclidean distance, denoted by  $dist$ , between a missing sample  $S_{im'}^{miss}$ ,  $m' \in (1, 2, \dots, n)$  and one of nearest  $k$  samples  $S_{ij}^{near}$ :

$$r_j = \frac{1}{dist(S_{ij}, S_{im'}^{miss})}. \quad (5)$$

As shown in Fig. 1, the difference between the imputation of the training set and the test set is that we do not recluster the test set from scratch. Instead, the KMeans model trained on the training set is used to predict pseudo-labels for the test set. The imputed data is then generated using clusters from the training set that share the same pseudo-labels as those predicted for the test set. The test set is solely utilized as a source of data requiring imputation.

### III. EXPERIMENTS

#### A. Datasets

**NTU-RGB+D 60/120 with occlusion.** The NTU-60/120 datasets provide skeleton sequences for action recognition with cross-subject (xsub) and cross-set/cross-view (xset/xview) evaluation settings. Two occlusion types are used: synthesized realistic occlusion based on 3D furniture projections and random occlusion where 20% of coordinates are randomly obscured. Evaluation Protocols: **Linear Eval:** Train a supervised linear classifier on a frozen encoder using imputed data. **Semi-supervised:** Pre-train encoder on imputed data, then fine-tune full model using 1% or 10% labeled data. **Finetune:** Attach classifier to encoder, finetune entire network on imputed data.

#### B. Evaluation of KNN Imputation

To demonstrate the effectiveness of our imputation method, we compare it with the non-imputed NTU-60/120 with realistic occlusion. As shown in Tables I, II, and III, almost all three downstream task performances of all the investigated methods have shown promising improvements on the imputed NTU-60/120 dataset, shown in our imputed  $\Delta$  part.

#### C. Evaluation of OPSTL framework

We conduct a series of comparison experiments to evaluate OPSTL on this new challenge proposed by this work. As shown in Tables I, II, and III, for all the non-imputed, randomly imputed, and KNN-imputed NTU-60/120, OPSTL outperforms the current state-of-the-art method PSTL on linear evaluation. OPSTL is improved by 1.59% and 1.95% on xsub and xview of NTU-60 with realistic occlusion, respectively. In addition, OPSTL achieves a performance gain of 1.47% and 2.28% on xsub and xset of NTU-120 with realistic occlusion. OPSTL achieves not only improvements on the non-imputed dataset but also on the imputed NTU-60/120 dataset.

TABLE I: Linear evaluation results on **NTU-60** with synthesized realistic occlusion, randomly imputed values, and imputed values by our proposed method. “ $\Delta$ ” represents the difference compared to the non-imputed NTU-60. **J** and **M** represent the joint stream and the motion stream.

Method	Stream	Occluded (%)		Randomly imputed (%)				Our imputed (%)			
		xsub acc.	xview acc.	xsub acc.	xview acc.	$\Delta$	xsub acc.	xview acc.	$\Delta$	xsub acc.	xview acc.
SkeletonCLR [30]	<b>J</b>	56.74	53.25	47.12	$\downarrow 9.62$	58.09	$\uparrow 4.84$	57.61	$\uparrow 0.87$	64.43	$\uparrow 11.18$
2s-CrosSCLR [30]	<b>J+M</b>	59.88	57.47	51.96	$\downarrow 7.92$	52.18	$\downarrow 5.29$	62.76	$\uparrow 2.88$	62.54	$\uparrow 5.07$
AimCLR [31]	<b>J</b>	58.90	55.21	6.36	$\downarrow 52.54$	53.91	$\downarrow 1.30$	63.40	$\uparrow 4.50$	56.68	$\uparrow 1.47$
PSTL [32]	<b>J</b>	59.52	63.60	62.18	$\uparrow 2.66$	67.97	$\uparrow 4.37$	<b>67.31</b>	$\uparrow 7.79$	71.10	$\uparrow 7.50$
<b>OPSTL (ours)</b>	<b>J</b>	<b>61.11</b>	<b>65.55</b>	<b>65.63</b>	$\uparrow 4.52$	<b>68.01</b>	$\uparrow 2.46$	67.11	$\uparrow 6.00$	<b>71.39</b>	$\uparrow 5.84$

TABLE II: Linear evaluation results on **NTU-120** dataset.

Method	Stream	Occluded (%)		Randomly imputed (%)				Our imputed (%)			
		xsub acc.	xset acc.	xsub acc.	xset acc.	$\Delta$	xsub acc.	xset acc.	$\Delta$	xsub acc.	xset acc.
SkeletonCLR [30]	<b>J</b>	44.93	42.78	44.42	$\downarrow 0.51$	40.12	$\downarrow 2.66$	48.63	$\uparrow 3.70$	45.06	$\uparrow 2.28$
2s-CrosSCLR [30]	<b>J+M</b>	49.63	48.14	39.11	$\downarrow 10.52$	33.77	$\downarrow 14.37$	49.58	$\downarrow 0.05$	54.43	$\uparrow 6.29$
AimCLR [31]	<b>J</b>	44.58	48.93	0.86	$\downarrow 43.72$	1.16	$\downarrow 47.77$	52.50	$\uparrow 7.92$	52.83	$\uparrow 3.90$
PSTL [32]	<b>J</b>	54.18	51.90	56.12	$\uparrow 1.94$	52.66	$\uparrow 0.76$	57.05	$\uparrow 2.87$	57.94	$\uparrow 6.04$
<b>OPSTL (ours)</b>	<b>J</b>	<b>55.65</b>	<b>54.18</b>	<b>56.43</b>	$\uparrow 0.78$	<b>53.90</b>	$\downarrow 0.28$	<b>59.29</b>	$\uparrow 3.64$	<b>58.25</b>	$\uparrow 4.07$

TABLE III: Finetune and Semi-supervised results on the imputed NTU-60/120 datasets.

Method	Stream	Imputed NTU-60 (%)				Imputed NTU-120 (%)			
		xsub acc.	xset acc.	xview acc.	$\Delta$	xsub acc.	xset acc.	xset acc.	$\Delta$
<b>Finetune:</b>									
SkeletonCLR [30]	<b>J</b>	70.58	$\uparrow 3.22$	80.76	$\uparrow 4.42$	63.17	$\uparrow 4.06$	62.12	$\uparrow 1.20$
2s-CrosSCLR [30]	<b>J+M</b>	72.94	$\uparrow 1.32$	80.34	$\uparrow 0.09$	65.06	$\uparrow 0.39$	67.45	$\uparrow 2.43$
AimCLR [31]	<b>J</b>	70.53	$\uparrow 0.44$	75.52	$\downarrow 3.21$	67.08	$\uparrow 5.25$	66.62	$\uparrow 1.91$
PSTL [32]	<b>J</b>	75.16	$\uparrow 2.48$	85.24	$\uparrow 2.05$	69.10	$\uparrow 1.20$	<b>69.42</b>	$\uparrow 2.71$
<b>OPSTL (ours)</b>	<b>J</b>	<b>75.43</b>	$\uparrow 2.41$	<b>86.01</b>	$\uparrow 1.92$	<b>70.89</b>	$\uparrow 2.21$	69.14	$\uparrow 1.89$
<b>Semi 1%:</b>									
SkeletonCLR [30]	<b>J</b>	31.99	$\uparrow 13.47$	31.18	$\uparrow 10.16$	20.45	$\uparrow 3.13$	16.24	$\uparrow 2.23$
2s-CrosSCLR [30]	<b>J+M</b>	32.66	$\uparrow 4.69$	31.18	$\uparrow 10.35$	19.38	$\uparrow 0.21$	20.12	$\uparrow 7.59$
AimCLR [31]	<b>J</b>	34.44	$\uparrow 5.28$	27.04	$\uparrow 8.92$	22.59	$\uparrow 6.13$	20.68	$\uparrow 5.38$
PSTL [32]	<b>J</b>	<b>40.81</b>	$\uparrow 7.99$	<b>39.61</b>	$\uparrow 13.06$	27.43	$\uparrow 5.92$	<b>25.52</b>	$\uparrow 6.52$
<b>OPSTL (ours)</b>	<b>J</b>	40.07	$\uparrow 6.48$	38.65	$\uparrow 10.76$	<b>27.90</b>	$\uparrow 4.69$	24.57	$\uparrow 4.71$
<b>Semi 10%:</b>									
SkeletonCLR [30]	<b>J</b>	55.97	$\uparrow 2.98$	60.83	$\uparrow 9.37$	44.37	$\uparrow 2.33$	42.68	$\uparrow 7.72$
2s-CrosSCLR [30]	<b>J+M</b>	59.17	$\uparrow 3.16$	59.01	$\uparrow 3.86$	46.89	$\uparrow 2.07$	48.24	$\uparrow 8.44$
AimCLR [31]	<b>J</b>	59.64	$\uparrow 2.30$	54.34	$\downarrow 0.36$	48.38	$\uparrow 6.25$	48.96	$\uparrow 3.63$
PSTL [32]	<b>J</b>	63.04	$\uparrow 4.41$	68.89	$\uparrow 7.54$	53.26	$\uparrow 2.80$	53.42	$\uparrow 4.14$
<b>OPSTL (ours)</b>	<b>J</b>	<b>64.04</b>	$\uparrow 5.26$	<b>70.04</b>	$\uparrow 6.22$	<b>54.71</b>	$\uparrow 2.90$	<b>53.50</b>	$\uparrow 3.38$

#### D. Ablation Study

1) To validate the effectiveness of the imputation method, we perform random imputation on NTU-60/120 with realistic occlusion. From Table I and Table II, it is obvious that our proposed imputation method outperforms random imputation on linear evaluation. The performances of SkeletonCLR, 2s-CrosSCLR, and AimCLR all deteriorate under random imputation. The most severe decline is observed in AimCLR, where the accuracy drops to nearly 1%. This clearly illustrates that random completion undermines the whole skeleton information, which is crucial for action recognition methods that leverage whole skeleton data.

On the contrary, in the case of methods that utilize partial skeleton sequences for representation learning, such as PSTL, there is still a slight improvement in accuracy despite the use of random imputation. However, for our proposed ASM, the improvement is minimal or even negative. For instance,

TABLE IV: Stepwise ablation results on realistic occluded and imputed NTU-120. Method<sup>1+2</sup> denotes two stages during the pre-training. **S1** is first stage and **S2** is second stage. All experiments are on the joint stream.

Method <sup>1+2</sup>	(S1) Occluded NTU-120 (%)		(S2) Imputed NTU-120 (%)	
	xsub	xset	xsub	xset
PSTL [32] + PSTL [32]	54.18	51.90	57.05	57.94
OPSTL (ours) + PSTL [32]	55.65	54.18	58.70	57.52
<b>OPSTL (ours) + OPSTL (ours)</b>	<b>55.65</b>	<b>54.18</b>	<b>59.29</b>	<b>58.25</b>

on xset of randomly imputed NTU-120, OPSTL experiences a reduction of 0.28% in accuracy compared to non-imputed data. Yet, it still outperforms the state-of-the-art PSTL. This observation underscores the fact ASM effectively utilizes high-quality data for representation learning.

2) To better illustrate the effectiveness of ASM, we conducted a stepwise ablation study on the NTU-120 dataset. As shown in Table IV, during the first stage of pre-training, we observed that using ASM yields accuracy improvements of 1.47% for xsub and 2.28% for xset over CSM. Building upon the ASM-based first stage, in the second stage, both CSM and ASM are employed. The results indicate in the second stage, continuing to use ASM yields gains of 0.59% for xsub and 0.73% for xset compared to using CSM.

3) To demonstrate the effectiveness of our imputation method on random occlusions, we validate it using OPSTL on the NTU-60/120 datasets. As shown in Table V, after the imputation, OPSTL exhibits significant improvements across various splits of the NTU-60/120 datasets.

TABLE V: Linear evaluation results of OPSTL on non-imputed and imputed NTU-60/120 with random occlusion. All experiments are on the joint stream.

Method	Randomly occluded NTU-60 (%)		Randomly occluded NTU-120 (%)	
	xsub	xview	xsub	xset
Non-Imputed	41.90	30.16	10.32	4.22
Imputed	47.31	55.29	23.54	18.59

#### IV. CONCLUSION

In this paper, we propose effective solutions for the challenges of self-supervised skeleton-based action recognition in occluded environments. First, we construct a large-scale occluded self-supervised skeleton-based human action recognition benchmark considering well-established approaches and propose the Adaptive Spatial Masking (ASM) data augmentation mechanism to formulate OPSTL framework. We introduce a skeleton data imputation method using KMeans and KNN, reducing computation overhead for occluded skeleton completion, named as KNN imputation. Experimental results validate the efficacy of our approach across various self-supervised approaches, empowering robots to perform robust action recognition in real-world occluded scenarios.



## REFERENCES

- [1] C. Bandi and U. Thomas, "Skeleton-based action recognition for human-robot interaction using self-attention mechanism," in *2021 16th IEEE International Conference on Automatic Face and Gesture Recognition (FG)*, 2021, pp. 1–8.
- [2] Z. Song, Z. Yin, Z. Yuan, C. Zhang, W. Chi, Y. Ling, and S. Zhang, "Attention-oriented action recognition for real-time human-robot interaction," in *2020 International Conference on Pattern Recognition (ICPR)*, 2020, pp. 7087–7094.
- [3] A. Sharghi, H. Haugerud, D. Oh, and O. Mohareri, "Automatic operating room surgical activity recognition for robot-assisted surgery," in *International Conference on Medical Image Computing and Computer Assisted Intervention (MICCAI)*, 2020, pp. 385–395.
- [4] V. Voronin, M. Zhdanova, E. Semenishchev, A. Zelenskii, Y. Cen, and S. Agaian, "Action recognition for the robotics and manufacturing automation using 3-D binary micro-block difference," *The International Journal of Advanced Manufacturing Technology*, vol. 117, pp. 2319–2330, 2021.
- [5] S. Danafar and N. Gheisari, "Action recognition for surveillance applications using optic flow and svm," in *Asian Conference on Computer Vision (ACCV)*, vol. 4844, 2007, pp. 457–466.
- [6] Y. Du, Y. Fu, and L. Wang, "Skeleton based action recognition with convolutional neural network," in *2015 IAPR Asian Conference on Pattern Recognition (ACPR)*, 2015, pp. 579–583.
- [7] Q. Ke, M. Bennamoun, S. An, F. Sohel, and F. Boussaid, "A new representation of skeleton sequences for 3D action recognition," in *2017 IEEE Conference on Computer Vision and Pattern Recognition (CVPR)*, 2017, pp. 4570–4579.
- [8] M. Liu, H. Liu, and C. Chen, "Enhanced skeleton visualization for view invariant human action recognition," *Pattern Recognition*, vol. 68, pp. 346–362, 2017.
- [9] L. Shi, Y. Zhang, J. Cheng, and H. Lu, "Two-stream adaptive graph convolutional networks for skeleton-based action recognition," in *2019 IEEE/CVF Conference on Computer Vision and Pattern Recognition (CVPR)*, 2019, pp. 12018–12027.
- [10] C. Si, W. Chen, W. Wang, L. Wang, and T. Tan, "An attention enhanced graph convolutional LSTM network for skeleton-based action recognition," in *2019 IEEE/CVF Conference on Computer Vision and Pattern Recognition (CVPR)*, 2019, pp. 1227–1236.
- [11] Z. Chen, S. Li, B. Yang, Q. Li, and H. Liu, "Multi-scale spatial temporal graph convolutional network for skeleton-based action recognition," in *AAAI Conference on Artificial Intelligence (AAAI)*, vol. 35, no. 2, 2021, pp. 1113–1122.
- [12] Y. Du, W. Wang, and L. Wang, "Hierarchical recurrent neural network for skeleton based action recognition," in *2015 IEEE Conference on Computer Vision and Pattern Recognition (CVPR)*, 2015, pp. 1110–1118.
- [13] S. Song, C. Lan, J. Xing, W. Zeng, and J. Liu, "Spatio-temporal attention-based LSTM networks for 3D action recognition and detection," *IEEE Transactions on Image Processing*, vol. 27, no. 7, pp. 3459–3471, 2018.
- [14] P. Zhang, C. Lan, J. Xing, W. Zeng, J. Xue, and N. Zheng, "View adaptive neural networks for high performance skeleton-based human action recognition," *IEEE Transactions on Pattern Analysis and Machine Intelligence*, vol. 41, no. 8, pp. 1963–1978, 2019.
- [15] K. Peng, J. Fu, K. Yang, D. Wen, Y. Chen, R. Liu, J. Zheng, J. Zhang, M. S. Sarfraz, R. Stiefelhofen, and A. Roitberg, "Referring atomic video action recognition," in *European Conference on Computer Vision (ECCV)*, 2024.
- [16] Y. Wei, K. Peng, A. Roitberg, J. Zhang, J. Zheng, R. Liu, Y. Chen, K. Yang, and R. Stiefelhofen, "Elevating skeleton-based action recognition with efficient multi-modality self-supervision," in *2024 IEEE International Conference on Acoustics, Speech and Signal Processing (ICASSP)*, 2024, pp. 6040–6044.
- [17] N. Heidari and A. Iosifidis, "Progressive spatio-temporal graph convolutional network for skeleton-based human action recognition," in *2021 IEEE International Conference on Acoustics, Speech and Signal Processing (ICASSP)*, 2021, pp. 3220–3224.
- [18] A. Sabater, L. Santos, J. Santos-Victor, A. Bernardino, L. Montesano, and A. C. Murillo, "One-shot action recognition in challenging therapy scenarios," in *2021 IEEE/CVF Conference on Computer Vision and Pattern Recognition Workshops (CVPRW)*, 2021, pp. 2771–2779.
- [19] H. Yan, B. Hu, G. Chen, and E. Zhengyuan, "Real-time continuous human rehabilitation action recognition using OpenPose and FCN," in *2020 3rd International Conference on Advanced Electronic Materials, Computers and Software Engineering (AEMCSE)*, 2020, pp. 239–242.
- [20] M. B. Shaikh and D. Chai, "RGB-D data-based action recognition: A review," *Sensors*, vol. 21, no. 12, p. 4246, 2021.
- [21] K. Simonyan and A. Zisserman, "Two-stream convolutional networks for action recognition in videos," in *Advances in Neural Information Processing Systems (NeurIPS)*, vol. 27, 2014, pp. 568–576.
- [22] A. Ullah, J. Ahmad, K. Muhammad, M. Sajjad, and S. W. Baik, "Action recognition in video sequences using deep bi-directional LSTM with CNN features," *IEEE Access*, vol. 6, pp. 1155–1166, 2017.
- [23] H. H. Pham, L. Khoudour, A. Crouzil, P. Zegers, and S. A. Velastin, "Video-based human action recognition using deep learning: A review," *arXiv preprint arXiv:2208.03775*, 2022.
- [24] Z. Zhang, "Microsoft kinect sensor and its effect," *IEEE MultiMedia*, vol. 19, no. 2, pp. 4–10, 2012.
- [25] Z. Cao, T. Simon, S.-E. Wei, and Y. Sheikh, "Realtime multi-person 2D pose estimation using part affinity fields," in *2017 IEEE Conference on Computer Vision and Pattern Recognition (CVPR)*, 2017, pp. 1302–1310.
- [26] G. Hua, H. Liu, W. Li, Q. Zhang, R. Ding, and X. Xu, "Weakly-supervised 3D human pose estimation with cross-view U-shaped graph convolutional network," *IEEE Transactions on Multimedia*, vol. 25, pp. 1832–1843, 2023.
- [27] X. Liu, F. Zhang, Z. Hou, L. Mian, Z. Wang, J. Zhang, and J. Tang, "Self-supervised learning: Generative or contrastive," *IEEE Transactions on Knowledge and Data Engineering*, vol. 35, no. 1, pp. 857–876, 2023.
- [28] G. Kahn, A. Villaflor, B. Ding, P. Abbeel, and S. Levine, "Self-supervised deep reinforcement learning with generalized computation graphs for robot navigation," in *2018 IEEE International Conference on Robotics and Automation (ICRA)*, 2018, pp. 5129–5136.
- [29] L. Lin, S. Song, W. Yang, and J. Liu, "MS2L: Multi-task self-supervised learning for skeleton based action recognition," in *ACM International Conference on Multimedia (MM)*, 2020, pp. 2490–2498.
- [30] L. Li, M. Wang, B. Ni, H. Wang, J. Yang, and W. Zhang, "3D human action representation learning via cross-view consistency pursuit," in *2021 IEEE/CVF Conference on Computer Vision and Pattern Recognition (CVPR)*, 2021, pp. 4741–4750.
- [31] T. Guo, H. Liu, Z. Chen, M. Liu, T. Wang, and R. Ding, "Contrastive learning from extremely augmented skeleton sequences for self-supervised action recognition," in *AAAI Conference on Artificial Intelligence (AAAI)*, vol. 36, no. 1, 2022, pp. 762–770.
- [32] Y. Zhou, H. Duan, A. Rao, B. Su, and J. Wang, "Self-supervised action representation learning from partial spatio-temporal skeleton sequences," in *AAAI Conference on Artificial Intelligence (AAAI)*, 2023, pp. 3825–3833.
- [33] J. Zbontar, L. Jing, I. Misra, Y. LeCun, and S. Deny, "Barlow twins: Self-supervised learning via redundancy reduction," in *International Conference on Machine Learning (ICML)*, vol. 139, 2021, pp. 12310–12320.
- [34] K. Peng, A. Roitberg, K. Yang, J. Zhang, and R. Stiefelhofen, "Delving deep into one-shot skeleton-based action recognition with diverse occlusions," *IEEE Transactions on Multimedia*, vol. 25, pp. 1489–1504, 2023.
- [35] T. M. Cover and P. E. Hart, "Nearest neighbor pattern classification," *IEEE Transactions on Information Theory*, vol. 13, no. 1, pp. 21–27, 1967.
- [36] T. Kanungo, D. M. Mount, N. S. Netanyahu, C. D. Piatko, R. Silverman, and A. Y. Wu, "An efficient k-means clustering algorithm: analysis and implementation," *IEEE Transactions on Pattern Analysis and Machine Intelligence*, vol. 24, no. 7, pp. 881–892, 2002.
- [37] J. K. Dixon, "Pattern recognition with partly missing data," *IEEE Transactions on Systems, Man, and Cybernetics*, vol. 9, no. 10, pp. 617–621, 1979.
- [38] F. Pedregosa, G. Varoquaux, A. Gramfort, V. Michel, B. Thirion, O. Grisel, M. Blondel, P. Prettenhofer, R. Weiss, V. Dubourg, J. Vanderplas, A. Passos, D. Cournapeau, M. Brucher, M. Perrot, and E. Duchesnay, "Scikit-learn: Machine learning in python," *Journal of Machine Learning Research*, vol. 12, pp. 2825–2830, 2011.